Published in Journal of the Optical Society of America B 22, issue 2, 481-487, 2005
which should be used for any reference to this work

Analysis of the phonon-polariton response of silicon carbide microparticles and nanoparticles by use of the boundary element method

Carsten Rockstuhl, Martin G. Salt, and Hans P. Herzig

University of Neuchâtel, Institute of Microtechnology, Rue Breguet 2, CH-2000 Neuchâtel, Switzerland

We investigate the small-particle phonon-polariton response of several microstructures that are made of silicon carbide (SiC). Phonon polaritons can be excited in a wavelength region between 10 and 12 μm. Simple structures such as elliptical cylinders support phonon polaritons at two wavelengths, which depend on the axis ratio of the particle. In particles with a more irregular shape such as rectangular or triangular cylinders, up to five phonon polaritons can be excited. Through comparison of the strength of phonon-polariton excitation with the similar effect of the plasmon-polariton excitation in metallic nanoparticles, it is found that the excitation of phonon polaritons is more efficient. This behavior is attributed to the lower imaginary part of the dielectric constant of SiC.

1. INTRODUCTION

Silicon carbide (SiC) is a material that has recently attracted interest owing to its applications as a wide-bandgap semiconductor used for high-temperature and high-power microelectronics. For example, it can be applied to a Schottky contact[1] or as the emitting material in a blue laser diode.[2] Another interesting property of the material is its special dielectric constant in the far-infrared region of the spectrum between 10 and 12 μm.[3,4] In this spectral region the real part has a negative value between -1 and -10, and the imaginary part is very small. This dielectric function is comparable with that of metals, such as silver in the blue part and gold in the green part of the spectrum.[5] Illumination of small particles made of these metallic materials at the appropriate wavelengths will excite a surface plasmon, which is a collective oscillation of the free electrons.[6] Nevertheless, the physical origin is hidden behind the dielectric constant, and the physical interpretation of the behavior is based on arguments from solid-state physics. The frequency of the driving illumination wave field equals the oscillating eigenfrequency of the free electrons in the metallic bulk material, and the movement of the electrons becomes resonant. In SiC the free electrons play only a minor role, but the frequency of the illuminating wave field might instead match the resonance frequency of the Si and C sublattices,[7] and a small-particle phonon polariton is thus excited. This excitation leads to an enhanced field amplitude in the vicinity of the particle (near field) and to a strong scattering cross section (SCS) at the resonance wavelength. The first investigations of the resonant scattering behavior in the infrared region of the spectrum for SiC were made for the detection of the mass outflow of carbon stars and meteorites.[8] In addition, this unique property of SiC found an interesting application as a coherent, directed emitter in the corresponding spectral region.[9,10]

Experimental investigations of excited phonon polaritons at nanometer- and micrometer-sized SiC particles attracted the interest of some researchers. For example, Hillenbrand *et al.*[11] measured the field distribution in the vicinity of microstructures made of SiC with a scanning near-field optical microscope. They applied electrostatic theory to compare the resonance behavior of particles made of SiC with particles made of silver and gold. Anderson[12] showed that the excitation of phonon resonances in small spheres made of SiC will lead to an enhanced infrared absorbtion for molecules attached to the surface of the particles if the illumination wavelength is chosen to be equal to the phonon resonance wavelength.

SiC particles can be used as a complement for metallic particles in various recently developed optical devices designed, e.g., for the guiding of light,[13] filter applications,[14] or an optical data-storage system.[15] A significant advantage of the use of SiC instead of metals is its smaller imaginary part in the dielectric constant.[11] This will result in a weaker damping and a corresponding sharper resonance. A quantum cascaded laser that emits in the appropriate spectral region could be used[16] as the light source for the different applications. In addition, SiC offers the advantage that environmental conditions affect the lattice parameters, resulting in a change in the phonon-polariton spectrum. This enables a broad range of sensor-type applications for the detection of changing environmental parameters, such as temperature or pressure. However, for all these applications, it is first necessary to understand in detail the characteristics of the phonon-polariton resonance in SiC particles. As the geometrical shape of the scatterer is one of the major parameters, that influences the phonon-polariton response, we will present a detailed study of the excitation of small-particle phonon polaritons in cylindrical particles made of 6H-SiC as a function of the geometrical cross section. The cylinders have an infinite extension in the third di-

mension. These calculations serve as a preliminary analysis for an experimental investigation that is currently in progress. The structures that are currently fabricated are essentially one-dimensional gratings, which corresponds to the simulated situation.

The numerical method used to analyze the scattering properties is the boundary element method (BEM).[17] A detailed description of the method can be found in Ref. 18. We will start our investigation in analyzing the simplest structures: circular and elliptical cylinders. Such particles exhibit two resonance wavelengths. Illumination of the particle under an angle will excite both phonon polaritons. It will be shown that the resonance wavelength can be tuned when the axis ratio of the elliptical particles, is changed. The strength can be tuned when the size of the particles is changed at a constant axis ratio. Additionally we will analyze objects that exhibit a more complicated phonon-polariton response, like rectangular and triangular cylinders. Their phonon-polariton response is split into a band that are all excited independent of the illumination direction. Finally, we will compare the excitation of phonon polaritons with the excitation of plasmon polaritons in metallic nanoparticles.

2. RESPONSE OF CIRCULAR AND ELLIPTICAL CYLINDERS

The simplest structure that can be analyzed is a circular cylinder. Figure 1 shows the SCS as a function of the wavelength for a circular scatterer with a radius of $r = 500\,\mathrm{nm}$. Excitation of phonon polaritons is only possible with TM-polarized light, which means that the magnetic field oscillates parallel to the cylinder. For all structures, we have calculated the magnitude of the near-field amplitude distribution (illuminating amplitude is unity) to visualize the excited-surface phonon polaritons (H_z component of the electromagnetic field) and the SCS as defined in Ref. 19. Because the scattering problem consists of a plane wave incident on an infinite circular cylinder, Mie theory exists as a quasianalytical solution, and we can compare the results obtained from the BEM with the correct solution[20] to verify implementation of the BEM. It can be seen that the results for both theories

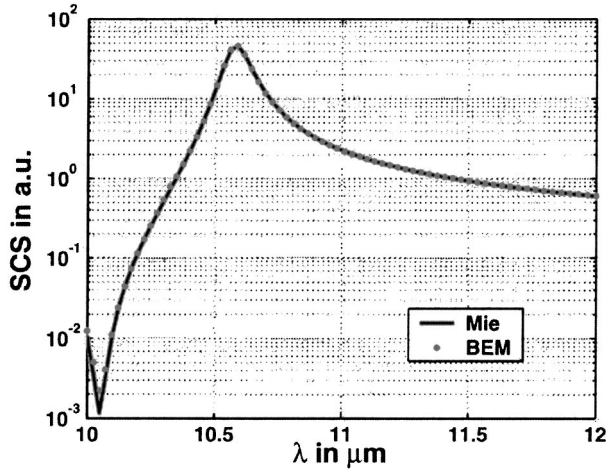

Fig. 1. SCS of a SiC circular cylinder with $r = 500\,\mathrm{nm}$ calculated with BEM and Mie theory.

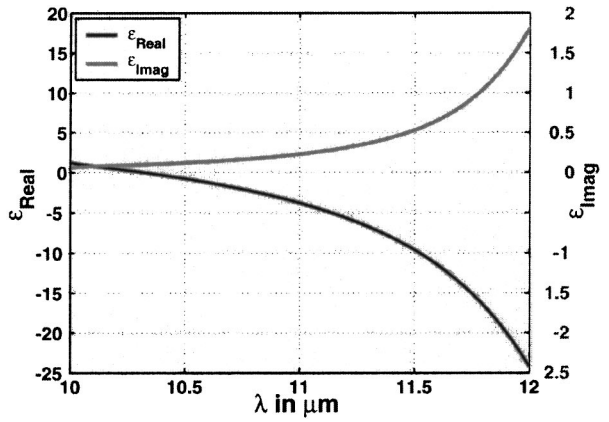

Fig. 2. Real and imaginary parts of the dielectric constant of SiC.

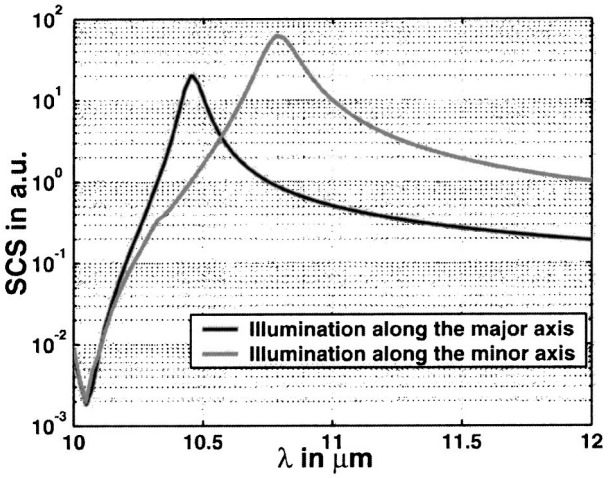

Fig. 3. SCS of a SiC elliptical cylinder with $r_1 = 630\,\mathrm{nm}$ and $r_2 = 315\,\mathrm{nm}$.

are in excellent agreement, and a sharp maximum in the SCS appears at 10.6 μm. A resonance is excited if the dielectric constant approaches a value of -1. The resonance wavelength corresponds to the local maximum of the SCS. In Fig. 2 the dielectric constant of 6H-SiC that was assumed in the calculation is shown.[21] These values were used for all calculations in this paper. At a wavelength of 10.6 μm the dielectric constant of SiC is $-1.15 + i0.13$, which is close to the resonance condition. The slight redshift of the resonance wavelength (the real part is -1 at $\lambda = 10.55\,\mu$m) is due to the finite size of the cylinder and the nonzero imaginary part of the dielectric constant. The resonant excitation of the dipole will lead to an enhanced SCS within a small wavelength range. The imaginary part diminishes the singular behavior. This leads to a damping and broadening of the response.

After the circular cross section, the next simplest case is an elliptical cylinder. In Fig. 3, the SCS for an elliptical cylinder with a radius of the minor axis of $r_2 = 315\,\mathrm{nm}$ and a radius for the major axis of $r_1 = 630\,\mathrm{nm}$, illuminated along the two fundamental axes, is shown. Through illumination of the scatterer along its major axis (the **k** vector is parallel to the major axis), a dipole will be excited at a wavelength of 10.45 μm. If the

illumination direction is parallel to the minor axis, the dipole is excited at 10.78 μm. The near-field amplitudes for the phonon polaritons at the excitation wavelengths for which the SCS has its highest value are shown for the two illumination directions in Fig. 4. The arrow in the figure indicates the illumination direction, which is given by the **k** vector. The field distribution of the dipole is comparable with the circular cylinder at the resonance condition. In Fig. 5 the SCS upon illumination of the object at three different angles, which are not coincident with one of the principle axis, are shown. The angles are 22°, 45°, and 67° and are taken with respect to the major axis.

As an intrinsic geometrical property the elliptical particle will support the two phonon polaritons at the two different wavelengths of 10.45 and 10.78 μm. Through illumination of the structure at an angle, both phonon polaritons are excited. The strength of the excitation corresponds to the projection of the incoming wave vector on

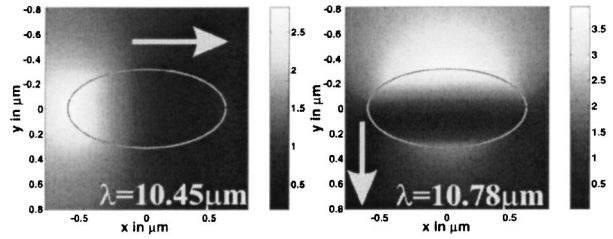

Fig. 4. Near-field amplitude around an elliptical cylinder (r_1 = 630 nm, r_2 = 315 nm) at the resonance wavelengths.

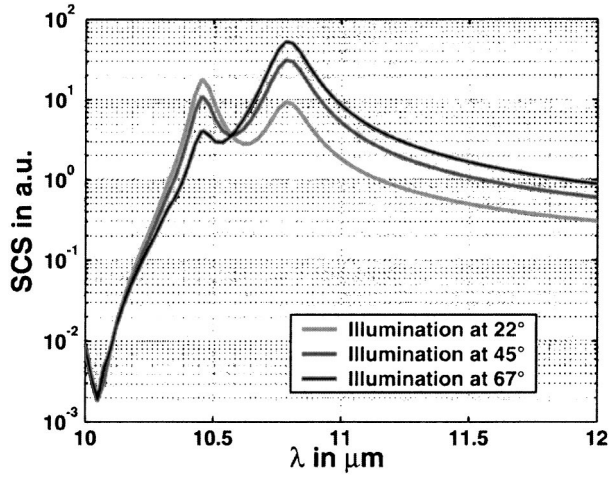

Fig. 5. SCS of a SiC elliptical cylinder with r_1 = 630 nm and r_2 = 315 nm for three different illumination directions.

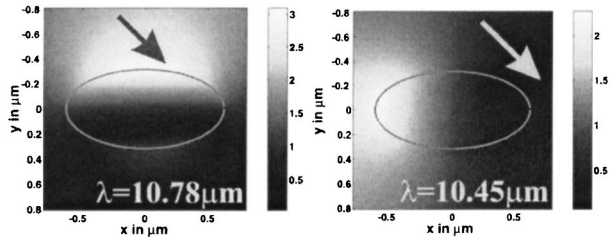

Fig. 6. Near-field amplitude around an elliptical cylinder (r_1 = 630 nm, r_2 = 315 nm) at the resonance wavelength for an illumination direction of 45°.

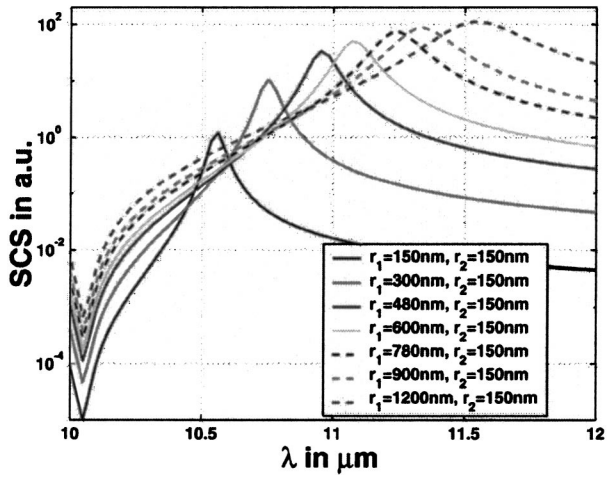

Fig. 7. SCS of an elliptical cylinder as a function of the axis ratio (from 1 to 8).

the two principal axes. In Fig. 6 the near-field distributions upon illumination of an elliptical particle at an angle of 45° are shown. The wavelength corresponds to the two maxima in the SCS. Obviously, the near fields are comparable with the field distributions of the two dipoles. These are excited if one illuminates the particle along its principal axis, as shown in Fig. 4. The only noticeable difference is a slight rotation and consequently an asymmetry in the field distributions.

3. TUNING THE RESONANCE WAVELENGTH OF AN ELLIPTICAL PARTICLE

For an elliptical particle, two resonances exist corresponding to the radii of the major and minor axes. This is a straightforward response that permits the tunability of the phonon-polariton wavelength in an effective way. A simple changing of the axis ratio of the particle enables the manipulation of the resonance behavior over a large wavelength range in an active manner. For sufficiently small particles, the size of the geometrical surface of the particle will not influence the resonance wavelength. Figure 7 shows the SCS for elliptical cylinders as a function of the axis ratio. The particles are illuminated along the minor axis. The minor axis is always 150 nm and the major axes are 150, 300, 480, 600, 780, 900, and 1200 nm. The different resonance wavelengths can be well discriminated in Fig. 7 and span a range of approximately 1 μm. It can be seen from Fig. 7 that an increase of the axis ratio also causes an increase of the FWHM. The FWHM changes from a value of 100 nm at an axis ratio of 1 to a full width of 500 nm at an axis ratio of 8. This is due to two effects. The first reason is a steady increase in the imaginary part of the dielectric constant at higher wavelengths (see Fig. 2). Another effect is an additional broadening and damping in the SCS if the geometrical size of the particles becomes larger. The field scattered by the particle suffers from phase retardation of the incoming wave front, broadening the SCS.

In summary, the wavelength at which the resonance occurs can be manipulated through a changing of the axis ratio of an elliptical particle. In Section 4 we will also

show how it is possible to control the strength of the resonance to balance the magnitude of the SCS for each of the particles.

4. TUNING THE RESONANCE STRENGTH OF AN ELLIPTICAL PARTICLE

In Fig. 8 the maximum of the SCS as a function of the radius for a circular cylinder is shown. The maximum is at $\lambda = 10.6\ \mu$m. For comparison, the strength of the SCS calculated through application of the quasistatic approximation is likewise shown in the figure.[20] For small particles the strength of the SCS scales with the fourth power of the radius, which makes it possible for one to tune the strength of the SCS in a controlled manner just by changing the size of the cylinder. The dipole wavelength remains constant for minute particles. For larger radii the strength as calculated with rigorous methods becomes weaker than is predicted by the electrostatic approximation. The origin of this effect is the phase retardation inside the particle that results in a damping of the total field by scattered field contributions that are out of phase. Such a rigorous calculation of the scattering strength as a function of the size can be done for all of the elliptical cylinders, and qualitatively the behavior is the same independent of the axis ratio. The wavelength for which the maximum in the SCS occurs remains fixed as long as the size of the particles does not become too large. An increase of the size will cause a redshift in the resonance wavelength for moderate particle radii.

The tunability of the strength of the SCS allows us to adjust the SCS for all the particles to an equal level by changing the size of the particles. Figure 9 shows the SCS on a linear scale for the particles with the same axis ratios as in Fig. 7 but with optimized overall size.

5. RESPONSE OF CYLINDERS WITH DIFFERENT CROSS SECTIONS

A. Rectangular Cylinder

To investigate geometries with a more complicated phonon-polariton response, we have analyzed a rectangular object with a size of 328 nm × 672 nm. For a simulation of more-realistic objects and to avoid numerical instabilities, we approximated the corners by circles with a radius of 40 nm. The SCS for two different illumination directions, which correspond to the axes of the particle, are shown in Fig. 10. Illumination of the rectangular cylinder along its short axis will excite a dominant dipole at 10.83 μm. A dipole for an illumination direction along the long axis is excited at 10.42 μm. Its amplitude is strongest on the illumination side, and the field on the backside is significantly lower. This resembles the behavior of the dipole excitation at an elliptical cylinder (Fig. 6). An additional higher multipole is excited at 10.70 μm. The near-field distributions for the resonances when the structure is illuminated along its long axis are shown in Fig. 11. Calculating all of the near-field amplitudes upon illumination of the object along the short axis reveals likewise the excitation of an additional higher multipoles at 10.42 μm. Nonetheless, the resonance strength is significantly lower than the strength of the dominant dipole. Figure 12 shows the near-field amplitudes for the excited phonon polaritons of the rectangular cylinder for an illumination direction along the short axis. For an estimation of the size dependence of

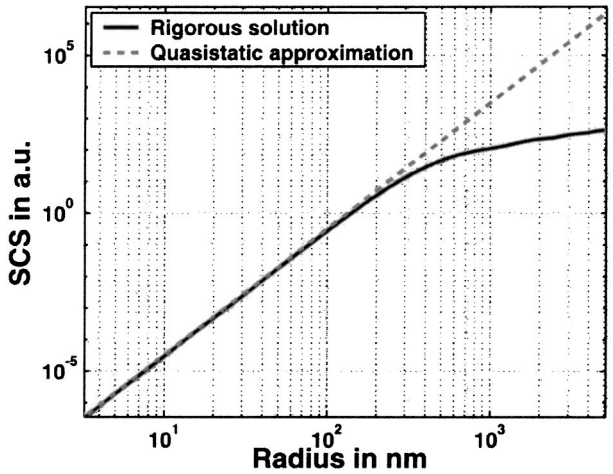

Fig. 8. Maximum of the SCS as a function of the radius for a circular cylinder ($\lambda = 10.6\ \mu$m).

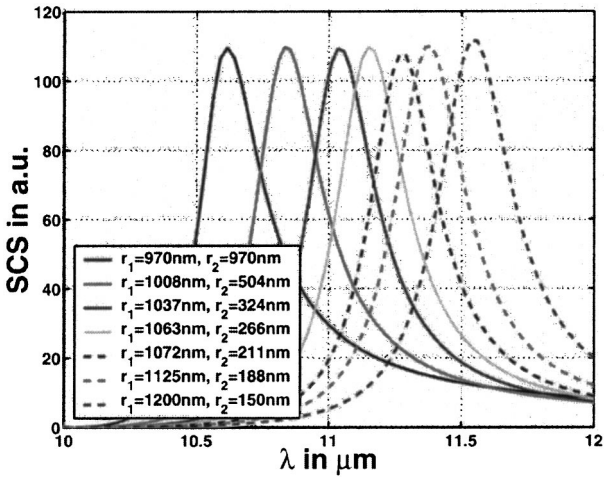

Fig. 9. SCS of an elliptical cylinder as a function of the radii.

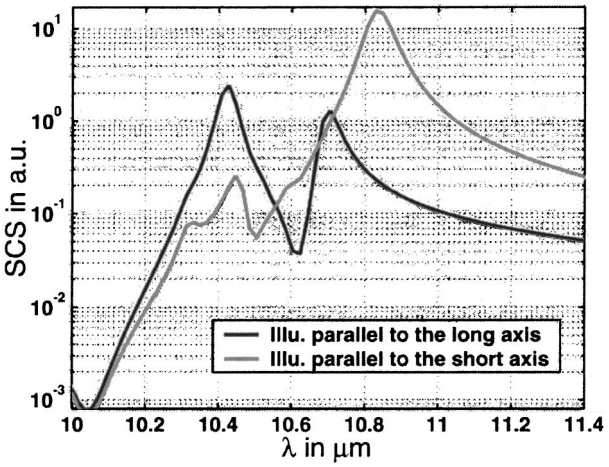

Fig. 10. SCS of a SiC rectangular cylinder with $a = 672$ nm and $b = 328$ nm.

the SCS, we have calculated the SCS for the same axis ratio but for different absolute sizes of the cylinder with an rectangular cross section. In Fig. 13 the SCS for three rectangular cylinders is shown. The inset rectangle and arrow indicate the illumination direction relative to the particle. The sizes are $a_1 = 672\,\text{nm}$, $b_1 = 328\,\text{nm}$; $a_2 = 1680\,\text{nm}$, $b_2 = 820\,\text{nm}$; and $a_3 = 3360\,\text{nm}$, $b_3 = 1640\,\text{nm}$. It can be seen that like the behavior of a circular cylinder, the resonance wavelengths remain approximately constant for moderate particle sizes. An excessive increase will produce a redshift of the spectra. The second important point that is comparable with the behavior of a circular cylinder is the increase of the half-width of the SCS for increasing particle sizes. As was shown for cylinders with an elliptical cross section, the resonance wavelength can be tuned over a certain range when the axis ratio of the particle is changed. Figure 14 shows the normalized SCS for a rectangular cylinder for three different axis ratios. The inset indicates the major axis; the length of the minor axis was kept constant at $b = 328\,\text{nm}$. The resonance wavelength can be well discriminated for the illumination along the short axis. The resonances for the illumination direction along the long axis remain constant to a good approximation. As one can see in the left part of Fig. 14, the only change occurs

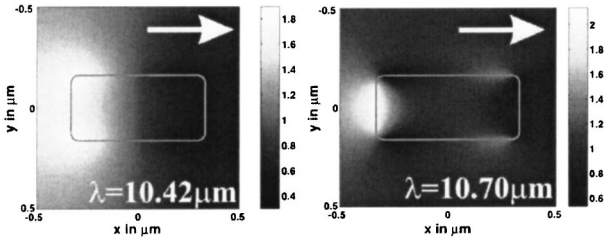

Fig. 11. Near-field amplitude around a rectangular cylinder ($a = 672\,\text{nm}$, $b = 328\,\text{nm}$) at the resonance wavelength for an illumination direction along the long axis.

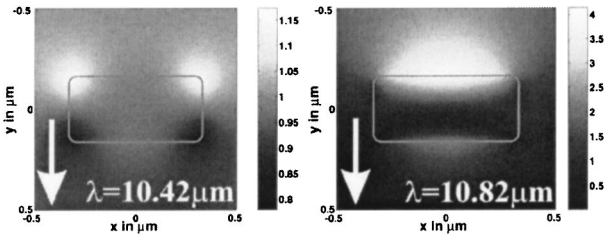

Fig. 12. Near-field amplitude around an rectangular cylinder ($a = 672\,\text{nm}$, $b = 328\,\text{nm}$) at the resonance wavelength for an illumination direction along the short axis.

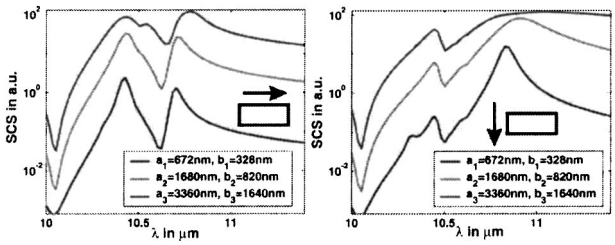

Fig. 13. SCS of a SiC rectangular cylinder with different sizes at the same axis ratio.

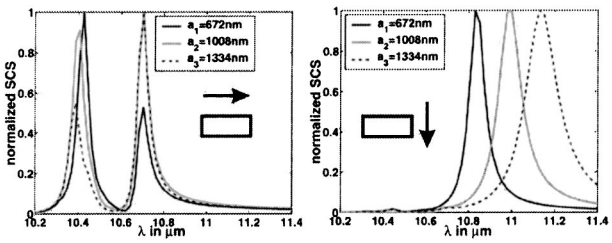

Fig. 14. Normalized SCS of a SiC rectangular cylinder for three different object sizes.

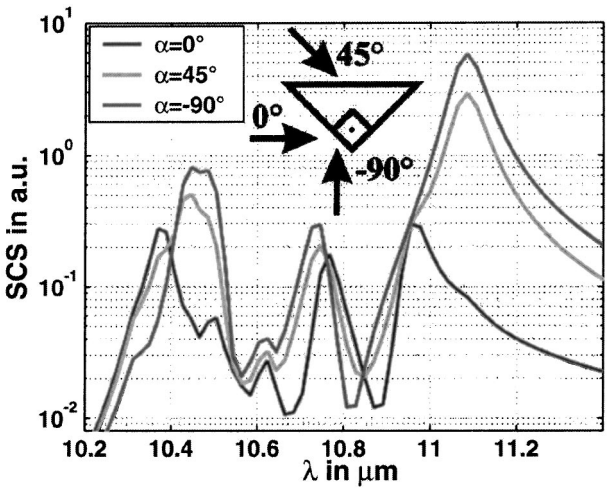

Fig. 15. SCS of a SiC triangular cylinder with $c = 848\,\text{nm}$ and $a = b = 600\,\text{nm}$.

in the amplitude ratio between the two resonances. From this and similar calculations we have found that the rectangular cylinder will always support the excitation of two phonon polaritons.

B. Triangular Cylinder

A further complicated structure is the triangular cylinder. We will treat here the special case of a right-angle triangle. The base c is 848 nm and $a = b = 600\,\text{nm}$. A similar round-off procedure for the corner of the triangular as for the rectangular cylinder was applied. The radius of the corner was 10 nm. The SCS of such an object for three different illumination directions is shown in Fig. 15. The geometry is shown in the inset of the figure. It can be seen that in good approximation five phonon polaritons are excited independent of the illumination direction. They are not present in the SCS for each illumination direction, because they are sometimes hidden behind the dominant contribution to the SCS of another phonon polariton, but calculation of the near fields reveals their existence. The single phonon polariton of a circular cylinder is split into a band of five phonon polaritons for a triangular cylinder. The near-field amplitude distributions of four excited phonon polaritons for the illumination direction of $-90°$ are shown in Fig. 16. Except for the phonon polariton excited at 11.08 μm, which is in good approximation a dipole, it becomes difficult to give the order of multipole for each of the phonon polaritons.

For the other illumination directions the field distributions appear similar to the fields as shown for the illumination direction of −90° and are omitted here.

6. COMPARING PHONON POLARITONS WITH PLASMON POLARITONS

A similar resonance effect that appears in metallic nanoparticles is the excitation of a plasmon polariton. Such an excitation will also cause an enhanced SCS and a large near-field amplitude. A plasmon polariton is a resonant oscillation of free electrons in the material, as outlined in Section 1, and appears in metals that have an appropriate negative dielectric constant in the visible part of the spectrum.

We used silver as the material in the simulations because of its lower imaginary part in the dielectric constant compared with other metals, such as gold or aluminum.[5] Two cardinal geometries, the circular and the quadratic cylinder, have been analyzed in terms of the scattering strength (by use of SCS) and the amplitude enhancement of the magnetic field on the surface of the particle. To eliminate the influence of the absolute size on the response, we present the results as a function of the wavelength divided by the radius of the circular cylinder or divided by the side length of the quadratic cylinder, respectively.

Figure 17(a) shows the SCS of a circular cylinder made of silver ($r_{\mathrm{Ag}} = 17.15\,\mathrm{nm}$) and made of silicon carbide ($r_{\mathrm{SiC}} = 530\,\mathrm{nm}$). It can be seen that the strength of the SCS for the particle made of SiC is nearly double the strength of the silver particle. The FWHM for the SiC cylinder is four times smaller than the FWHM for the particle made of silver, assuming a wavelength per radius as the unit. The effect is attributed to the significantly smaller imaginary part in the dielectric constant, as the geometry with respect to the wavelength is the same for the two cylinders. The imaginary part for silver at the plasmon wavelength of roughly 340 nm is approximately double the corresponding value for SiC at ∼10.6 μm and will cause a dampening and a broadening of the SCS. A similar behavior can be seen through analysis of the amplitude enhancement of the magnetic field directly at the surface of the particle. Results are shown in Fig. 17(b) again for the same circular cylinders. The difference in the amplitude enhancement is less pronounced, but the enhancement is still higher for the particle made of SiC. The FWHM is again smaller by a factor of four for the SiC particle than the corresponding value for silver.

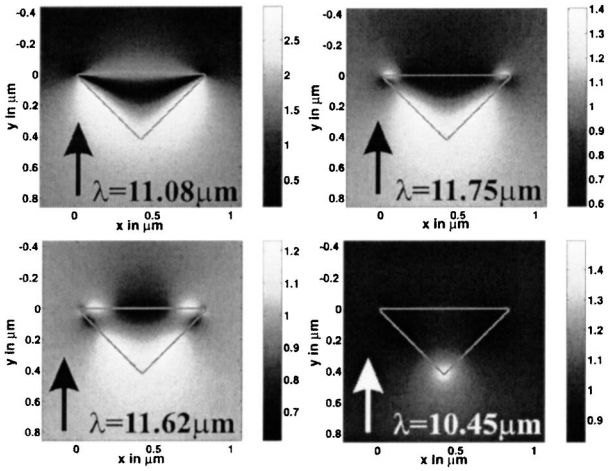

Fig. 16. Near-field amplitude around a triangular cylinder ($c = 848\,\mathrm{nm}$, $a = b = 600\,\mathrm{nm}$) at the resonance wavelength for the (11)-direction, as indicated by the arrow.

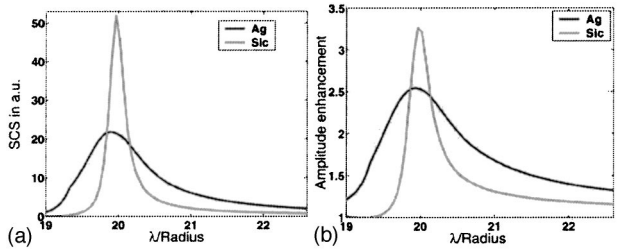

Fig. 17. Comparison of the SCS and the near-field amplitude enhancement of a circular cylinder made of Ag and SiC.

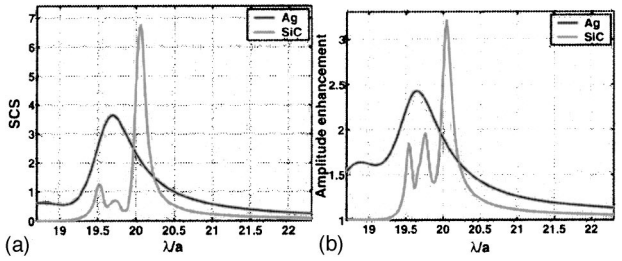

Fig. 18. Comparison of the SCS and the near-field amplitude enhancement of a quadratic cylinder made of Ag and SiC.

Similar results have been obtained by comparing the scattering response of quadratic cylinders made of SiC ($a = b = 535\,\mathrm{nm}$) and silver ($a = b = 18\,\mathrm{nm}$). The SCS and the field enhancement on the surface for these objects are shown in Figs. 18(a) and 18(b), respectively. Again, a difference in the strength and the FWHM for both the SCS and the field enhancement can be seen. The phonon polaritons are more efficiently excited, and their singular nature is more pronounced, owing to the lower imaginary part in the dielectric constant. Additionally, a splitting of the individual phonon polariton into three phonon polaritons is clearly observed. Such a splitting is attributed to the sharp corners in the geometry of the structure. The phonon polaritons are less strongly attenuated, whereas in silver the higher imaginary part in the dielectric constant will cause a broadening and damping, so that the fine structures do not appear in the spectrum. The spectrum is dominated by the dipole response associated with the basic quadratic cross section.

7. CONCLUSIONS

We have applied the BEM to the analysis of the small particle phonon-polariton excitation in 6H-SiC. Phonon polaritons are lattice vibrations that can be resonantly excited at appropriate wavelengths in the far-infrared part of the spectrum between 10 and 12 μm. Once a phonon polariton is excited, the energy that is scattered into the far-field amplitude as well as the near-field amplitude around the structure are enhanced. We have restricted the analysis to two-dimensional structures that are in-

variant in the third dimension. First, we calculated the scattering properties of circular and elliptical cylinders and discussed the different damping mechanisms. These cylinders will support phonon polaritons at distinguishable wavelengths that can be related to the axis ratio of the particle. Illumination of the cylinder under an angle that does not correspond to one of the principal axes will excite both resonances, but with a strength that corresponds to the projection of the incoming wavefield on the two principal axes. It was shown that the resonance wavelength can be tuned in a controlled manner when the axis ratio is changed. A change in the surface can control the scattering strength. Principally, we found that the SCS becomes broadened and redshifted for larger particles, independent of the geometrical cross section. For geometries other than elliptical, the single phonon polariton will be split into a band. Two phonon polaritons can be excited for rectangular cylinders, and five phonon polaritons can be excited for triangular cylinders.

By comparing the response of phonon polaritons excited in SiC and plasmon polaritons excited in silver, we have shown that the phonon polaritons are more efficiently excited owing to the lower imaginary part in the dielectric constant. The singular nature of the phonon polaritons was more pronounced, and a fine structure for the quadratic cylinders associated with the sharp corners was revealed. Such a response was not found for particles made of silver. The imaginary part in the dielectric constant of silver is too high, which will cause a significant damping and broadening of the plasmon-polariton response compared with the response of SiC.

ACKNOWLEDGMENTS

This research was supported by the European Union within the framework of the Future and Emerging Technologies-Super Laser Array Memory program under grant IST-2000-26479. The authors would like to thank Wataru Nakagawa for a careful reading of this manuscript.

C. Rockstuhl's e-mail address is carsten.rockstuhl@unine.ch.

REFERENCES

1. L. Zheng, R. P. Joshi, and C. Fazi, "Effects of barrier height fluctuations and electron tunneling on the reverse characteristics of 6H-SiC Schottky contacts," J. Appl. Phys. **85**, 3701–3707 (1999).
2. G. Ziegler, P. Lang, D. Theis, and C. Weyrich, "Single crystal growth of SiC substrate material for blue light emitting diodes," IEEE Trans. Electron Devices **30**, 277–281 (1983).
3. K.-H. Lee, C. H. Park, B.-H. Cheong, and K. J. Chang, "First-principles study of the optical properties of SiC," Solid State Commun. **92**, 869–872 (1994).
4. W. J. Moore, R. T. Holm, M. J. Yang, and J. A. Freitas, Jr., "Infrared dielectric constant of cubic SiC," J. Appl. Phys. **78**, 7255–7258 (1995).
5. P. B. Johnson and R. W. Christy, "Optical constants of the noble metals," Phys. Rev. B **6**, 4370–4379 (1972).
6. J. P. Kottmann and O. J. F. Martin, "Influence of the cross section and the permittivity on the plasmon-resonance spectrum of silver nanowires," Appl. Phys. B **73**, 299–304 (2001).
7. H. Mutschke, A. C. Andersen, D. Clément, T. Henning, and G. Peiter, "Infrared properties of SiC particles," Astron. Astrophys. **345**, 187–202 (1999).
8. T. Bernatowicz, G. Fraundorf, T. Ming, E. Anders, B. Wopenka, E. Zinner, and P. Fraundorf, "Evidence for interstellar SiC in the Murray carbonaceous meteorite," Nature **330**, 728–730 (1987).
9. J. J. Greffet, R. Carminati, K. Joulain, J. P. Mulet, S. Mainguy, and Y. Chen, "Coherent emission of light by thermal sources," Nature **416**, 61–64 (2002).
10. J. Le Gall, M. Olivier, and J. J. Greffet, "Experimental and theoretical study of reflection and coherent thermal emissionby a SiC grating supporting a surface-phonon polariton," Phys. Rev. B **55**, 10105–10114 (1997).
11. R. Hillenbrand, T. Taubner, and F. Keilmann, "Phonon-enhanced lightmatter interaction at the nanometre scale," Nature **418**, 159–162 (2002).
12. M. S. Anderson, "Enhanced infrared absorption with dielectric nanoparticles," Appl. Phys. Lett. **83**, 2964–2966 (2003).
13. S. A. Maier, M. L. Brongersma, P. G. Kik, S. Meltzer, A. A. G. Requicha, and H. A. Atwater, "Plasmonics–a route to nanoscale optical devices," Adv. Mater. **13**, 1501–1505 (2001).
14. S. Linden, A. Christ, J. Kuhl, and H. Giessen, "Selective suppression of extinction within the surface plasmon resonance of gold nanoparticles," Appl. Phys. B **73**, 311–316 (2001).
15. H. Dittlbacher, J. R. Krenn, B. Lamprecht, A. Leitner, and F. R. Aussenegg, "Spectrally coded optical data storage by metal nanoparticles," Opt. Lett. **25**, 563–565 (2000).
16. J. Faist, F. Capasso, D. L. Sivco, C. Sirtori, A. L. Hutchinson, and A. Y. Cho, "Quantum cascade laser," Science **264**, 553–556 (1994).
17. A. Madrazo and M. Nieto-Vesperinas, "Scattering of electromagnetic waves from a cylinder in front of a conducting plane," J. Opt. Soc. Am. A **12**, 1298–1309 (1995).
18. C. Rockstuhl, M. Salt, and H. P. Herzig, "Application of the boundary-element method to the interaction of light with single and coupled metallic nanoparticles," J. Opt. Soc. Am. A **20**, 1969–1973 (2003).
19. M. Born and E. Wolf, *Principles of Optics* (Cambridge U. Press, 1999).
20. C. F. Bohren and D. R. Huffmann, *Absorption and Scattering of Light by Small Particles* (Wiley, New York, 1983).
21. E. Palik, *Handbook of Optical Constants of Solids* (Academic, San Diego, Calif., 1985).